HEMATOPOIESIS AND STEM CELLS

Thyroid hormone regulates hematopoiesis via the TR-KLF9 axis

Ying Zhang,[1-3,*] Yuanyuan Xue,[2,4,*] Chunwei Cao,[1,3,*] Jiaojiao Huang,[1,3] Qianlong Hong,[1,3] Tang Hai,[1,3] Qitao Jia,[1,3] Xianlong Wang,[1,3] Guosong Qin,[1,3] Jing Yao,[1,3] Xiao Wang,[1,3] Qiantao Zheng,[1,3] Rui Zhang,[1,3] Yongshun Li,[1,3] Ailing Luo,[1,3] Nan Zhang,[1,3] Guizhi Shi,[5] Yanfang Wang,[6] Hao Ying,[7] Zhonghua Liu,[3,8] Hongmei Wang,[1-3] Anming Meng,[3,9] Qi Zhou,[1-3] Hong Wei,[3,10] Feng Liu,[2,4] and Jianguo Zhao[1-3]

[1]State Key Laboratory of Stem Cell and Reproductive Biology, Institute of Zoology, Chinese Academy of Sciences, Beijing, China; [2]Savaid Medical School, University of Chinese Academy of Sciences, Beijing, China; [3]Chinese Swine Mutagenesis Consortium; [4]State Key Laboratory of Membrane Biology, Institute of Zoology, and [5]Laboratory Animal Center, Institute of Biophysics, Chinese Academy of Sciences, Beijing, China; [6]State Key Laboratory of Animal Nutrition, Institute of Animal Science, Chinese Academy of Agricultural Sciences, Beijing, China; [7]Key Laboratory of Food Safety Research, Institute for Nutritional Sciences, Shanghai Institutes for Biological Sciences, Chinese Academy of Sciences, Shanghai, China; [8]College of Life Science, Northeast Agricultural University of China, Harbin, China; [9]School of Life Sciences, Tsinghua University, Beijing, China; and [10]Department of Laboratory Animal Science, College of Basic Medical Sciences, Third Military Medical University, Chongqing, China

Key Points

- A severe hypothyroid pig model created by ENU mutagenesis manifests the clinical features of human patients.
- *KLF9* acts as a critical mediator between the thyroid axis and hematopoiesis.

Congenital hypothyroidism (CH) is one of the most prevalent endocrine diseases, for which the underlying mechanisms remain unknown; it is often accompanied by anemia and immunodeficiency in patients. Here, we created a severe CH model together with anemia and T lymphopenia to mimic the clinical features of hypothyroid patients by ethylnitrosourea (ENU) mutagenesis in Bama miniature pigs. A novel recessive c.1226A>G transition of the dual oxidase 2 (*DUOX2*) gene was identified as the causative mutation. This mutation hindered the production of hydrogen peroxide (H_2O_2) and thus contributed to thyroid hormone (TH) synthesis failure. Transcriptome sequencing analysis of the thymuses showed that Krüppel-like factor 9 (*KLF9*) was predominantly downregulated in hypothyroid mutants. *KLF9* was verified to be directly regulated by TH in a TH receptor (TR)-dependent manner both in vivo and in vitro. Furthermore, knockdown of *klf9* in zebrafish embryos impaired hematopoietic development including erythroid maturation and T lymphopoiesis. Our findings suggest that the TR-KLF9 axis is responsible for the hematopoietic dysfunction and might be exploited for the development of novel therapeutic interventions for thyroid diseases. (*Blood*. 2017; 130(20):2161-2170)

Introduction

Congenital hypothyroidism (CH) is caused by thyroid hormone (TH) deficiencies. CH is one of the most prevalent endocrine diseases, occurring in 1 of 1400 to 2800 newborns.[1] Although CH can be treated by the administration of oral thyroxine after early diagnosis, a significant number of patients requiring TH replacement are unsatisfied with the therapy.[2] Therefore, a better understanding of the pathology of CH is required for the development of novel therapeutic interventions.

In general, TH deficiencies are associated with not only intellectual disabilities and growth retardation but also a strikingly high prevalence of anemia[3-5] and immunodeficiency of typical clinical features.[6-8] Based on anemia often being the first sign of hypothyroidism, accounting for 20% to 60% in hypothyroid patients, the current clinical guidelines recommend evaluating thyroid function in the workup of anemia.[9,10] Generally, the biological activities of TH are mainly mediated by tri-iodothyronine (T3) binding to its nuclear receptors (TH receptors [TRs]), which act as ligand-inducible transcription factors and modulate target gene expression in a hormone-dependent manner.[11,12] There are 2 forms of TRs, TRα and TRβ, encoded by the genes *THRA* and *THRB*, respectively, with differing tissue distributions.[13] A previous study[14] showed that TRα is essential for regulating erythropoiesis in $Thra^{-/-}$ mice. Moreover, TH deficiency impairs T- and B-lymphocyte development or hematopoietic system development in humans.[15-17] Although these studies offered some clues to the association between TH and hematopoiesis, the underlying mechanisms are not completely understood.

Pigs are excellent models for certain human diseases and have been extensively used in biomedical research.[18,19] Because of the many similarities in organ size, physiological characteristics, and, particularly, immunology[20,21] and TH metabolism[22] between pigs and humans, pigs are potentially useful CH disease models. To the best of our knowledge, no pig models of CH have been reported.

In this study, a Bama miniature pig line born with CH due to a homozygous missense mutation in the dual oxidase 2 (*DUOX2*) gene was generated by ethylnitrosourea (ENU) mutagenesis. The mutant

Submitted 4 May 2017; accepted 6 September 2017. Prepublished online as *Blood* First Edition paper, 25 September 2017; DOI 10.1182/blood-2017-05-783043.

*Y.Z., Y.X., and C.C. contributed equally to this study.

The online version of this article contains a data supplement.

There is an Inside *Blood* Commentary on this article in this issue.

The publication costs of this article were defrayed in part by page charge payment. Therefore, and solely to indicate this fact, this article is hereby marked "advertisement" in accordance with 18 USC section 1734.

pigs display phenotypic hallmarks of severe CH together with anemia and T lymphopenia. We further demonstrated that *KLF9* is regulated by the TH/TR axis and functions as an essential regulator of developmental hematopoiesis. The current study identifies a novel mechanism for TH-dependent disorders leading to anemia and immunodeficiency.

Methods

Animals

The Bama miniature pigs were raised at the Beijing Farm Animal Research Center (Institute of Zoology, Chinese Academy of Sciences) and had ad libitum access to a commercial pig diet (nutrient levels based on US National Research Council recommendations) and water throughout the experiment. The founder Bama miniature pigs carrying the D409G mutation were generated in a large-scale ENU mutagenesis screen.[23] Zebrafish strains including the Tubingen strain and the transgenic lines *gata1*:*dsRed* and *coro1a*:*GFP* were raised in system water at 28.5°C. All experiments involving animals were approved by the institutional animal care and use committee of the Institute of Zoology, Chinese Academy of Sciences.

Whole-genome sequencing and genotyping

Genomic DNA was isolated from the ear tissues using phenol/chloroform extraction, and whole-genome single-nucleotide polymorphism (SNP) genotyping was performed using porcine SNP60 BeadChips (Illumina, San Diego, CA) containing 62,163 SNP markers (for more details, please see the supplemental Methods, available on the *Blood* Web site).

MO, microinjection, and whole-mount in situ hybridization

The *klf9*-ATG morpholino (MO) sequence is 5′-TGCTGCAATATC TACGTCCGTCATC-3′. Stock solutions of 1 mM MO were prepared in double-distilled H_2O, and 6 ng of MO was injected into 1-cell stage embryos. The probes used for in situ hybridization in this study, including *klf9*, *thraa*, *thrab*, and *thrb*, are listed in supplemental Table 1. *cmyb*, *scl*, *lyz*, *be2-globin*, *gata1*, and *mfap4* were synthetized as previously reported.[24]

Statistical analysis

The unpaired 2-tailed Student *t* test (for 2 groups) and 1-way analysis of variance with Bonferroni post hoc test for multiple comparisons were performed for parametric data using GraphPad Prism software (GraphPad, San Diego, CA) or SPSS software (SPSS, Chicago, IL). Otherwise, the Mann-Whitney *U* test or the Kruskal-Wallis test (followed by Dunn post hoc analysis for >2 groups) was applied for nonparametric data. The results are presented as the means ± standard deviation (SD) unless otherwise indicated. A value of $P < .05$ was considered statistically significant.

Results

Identification of pig mutants exhibiting severe CH with a novel point mutation in *DUOX2* from an ENU mutagenesis screen

In an effort to screen for recessive mutations related to growth and development, we carried out a 3-generation breeding protocol (supplemental Figure 1) from an ENU mutagenesis program in Bama miniature pigs.[23] In line Z0013, a G1 boar (005T118) backcrossed to 6 G2 sows produced 206 G3 offspring, of which 22.3% (21 males and 25 females) exhibited strikingly weak vitality and nude skin (Figure 1A) in an autosomal-recessive inheritance pattern (Figure 1B). The mutant neonates had normal body weights (supplemental Figure 2A) but lower body temperatures (supplemental Figure 2B).

To identify the causative gene in the Z0013 line, we performed a family-based genome-wide linkage study (GWLS) to map the chromosome regions cosegregating with the mutant phenotypes. A significant linkage peak between 120 Mb and 144 Mb on chromosome 1 (logarithm of odds ratio [LOD] > 5) (Figure 1C) containing >180 annotated genes was identified. A total of 3517 SNPs within the region were further identified by whole-genome sequencing (WGS). Consequently, the 3517 SNPs were narrowed down to 10 nonsynonymous mutations (supplemental Figure 2C; supplemental Table 2). Of the 10 missense mutations, only the novel point mutation c.1226A>G in *DUOX2* cosegregated with the mutant phenotype (Figure 1D-E; supplemental Table 2). This point mutation resulted in a conserved aspartic acid transition to glycine (D409G, hereafter referred to as $DUOX2^{D409G/D409G}$) in the peroxidase-like domain (Figure 1F).

Additionally, genotyping results of the c.1226A>G mutation in a total of 481 pigs, including line Z0013 pigs, other lines of Bama miniature pigs, and Large White and Landrace, showed that the G/G homozygous genotype was only found in the affected pigs from line Z0013 but not in the other Bama pigs or any other breeds (supplemental Figure 2D-E; supplemental Table 3). To further confirm the ENU-mutagenized phenotype resulting from the *DUOX2* mutation, we generated homozygous *DUOX2* knockout pigs using the clustered regularly interspaced short palindromic repeats (CRISPR)/CRISPR-associated protein 9 (Cas9) system (supplemental Figure 3A-C; supplemental Table 4). The aberrant neonates (pigs 5-6) both exhibited the same phenotype as $DUOX2^{D409G/D409G}$ pigs (supplemental Figure 3D). The genotyping results confirmed the homozygous deletion of *DUOX2* in these 2 aberrant neonates (supplemental Figure 3E-G). Together, these results strongly suggested that the D409G mutation in DUOX2 is the causative mutation in this mutant line.

The porcine *DUOX2* gene (GenBank ID: 397060) spans ~20 kb and comprises 31 exons that encode a 1545-aa protein (Figure 1E-F). The mutated site is evolutionarily conserved among distinct mammals (Figure 1G), indicating its vital role within this domain for the function of DUOX2. In the same functional domain as the D409G mutation located, the R376W and R434X mutations in DUOX2 (Figure 1F) were found previously[25,26] in patients with CH. These findings indicate the clinical application of the current pig models of the D409G mutation to study human CH.

CH is generally caused by disorders of TH synthesis with goiter formation.[27] As shown in Figure 1H, overt goiters were observed in $DUOX2^{D409G/D409G}$ pigs. Histological analysis showed that the thyroid glands from mutant pigs were dysplastic with poorly developed follicles as a result of highly proliferating epithelial cells and completely absent colloids, when compared with the thyroids from wild-type (WT) pigs (Figure 1I). Furthermore, significantly decreased serum THs of T3, thyroxine (T4), free T3 (FT3) and free T4 (FT4), and markedly increased thyroid-stimulating hormone (TSH), were observed in mutant pigs (Figure 1J), suggesting severe hypothyroidism occurred; these symptoms are commonly observed in patients with CH.[28] Given the results mentioned thus far in this section, we have generated a pig model of severe CH, which is caused by the D409G mutation in DUOX2 from a large-scale ENU mutagenesis screen.

The p.D409G mutation in DUOX2 is a loss-of-function mutation that impairs H_2O_2-producing activity

Porcine *DUOX2* messenger RNA (mRNA) is ubiquitous, but it is mostly abundant in the thyroids (Figure 2A), suggesting that it has a unique role in thyroid function. Because the D409G mutation is located in the peroxidase-like domain, which is essential for the H_2O_2-generating activity of DUOX2,[29] we analyzed the concentration

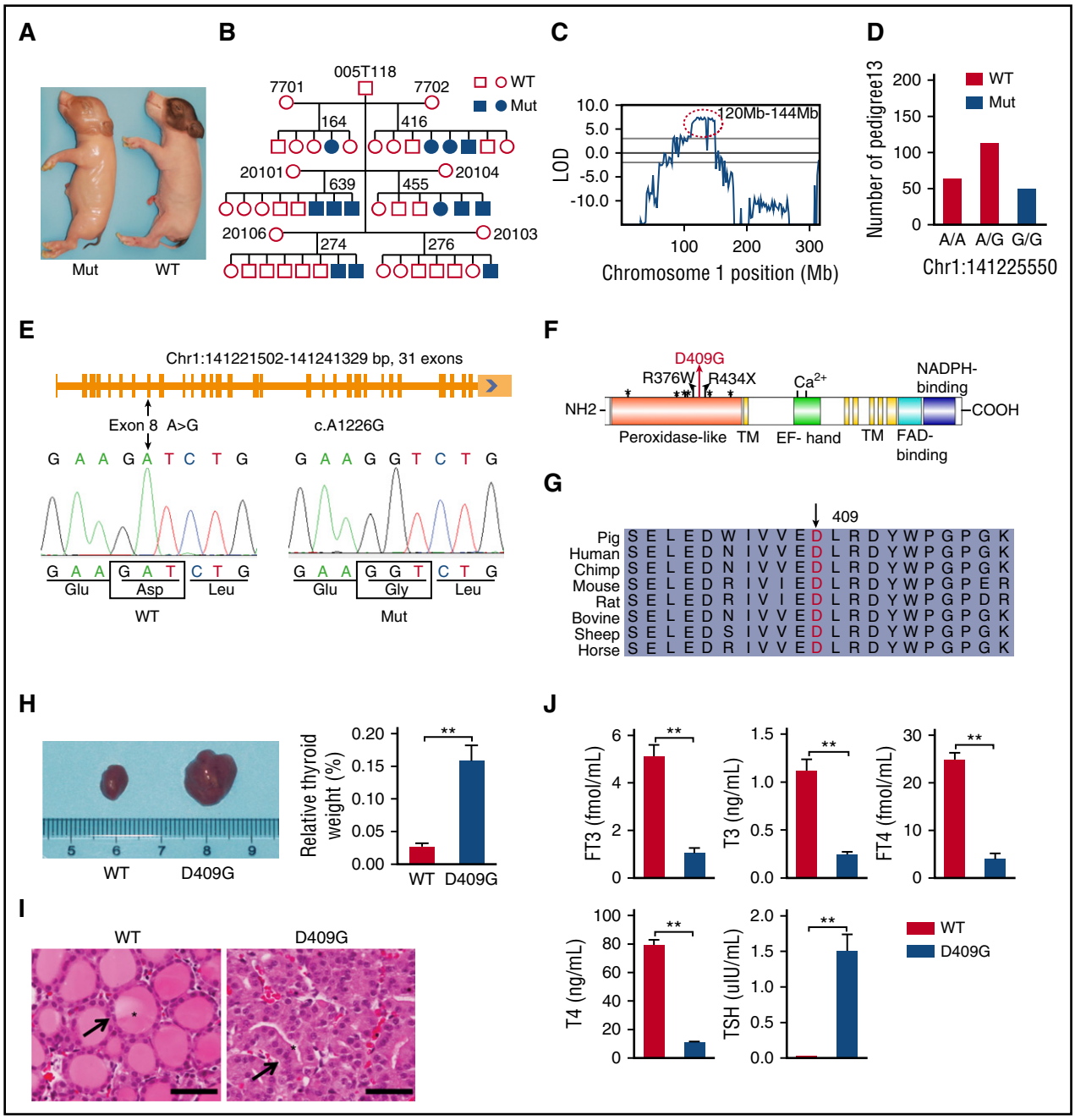

Figure 1. A mutant Bama miniature pig exhibiting the phenotype of severe CH was identified from a large-scale ENU mutagenesis screen. (A) A neonatal mutant compared with its littermate control. (B) The pedigree of the mutant family exhibiting an autosomal-recessive mode of inheritance. (C) A significant linkage peak between 120 Mb and 144 Mb on chromosome 1 was identified using a GWLS approach (LOD > 5). (D) A nucleotide A to G substitution in *DUOX2* was identified by WGS and cosegregated with the mutant phenotypes. (E) The porcine *DUOX2* gene is composed of 31 exons, and the mutation was located in exon 8 and resulted in a change of aspartic acid to glycine at position 409 (D409G) of the protein. (F) The D409G mutation (red arrow) is located in the peroxidase-like domain of DUOX2. The R376W and R434X mutations were found previously in patients with CH.[25,26] *, Glycosylation site. (G) The aspartic acid residue (arrow) in the D409G variant is highly conserved in mammalian DUOX2 proteins. (H) The thyroid glands of D409G pigs showed overt goiter formation at size and weight (WT, n = 7; D409G, n = 8; $^{**}P < .01$). (I) Sections of the thyroid glands were stained with hematoxylin and eosin (H&E). Follicles in the thyroids of D409G pigs lost their normal shape and became convoluted as a result of highly proliferating epithelial cells (black arrows) and completely disappearing colloids (asterisks) when compared with WT littermates. Scale bars, 50 μm. (J) The serum THs of T3, T4, FT3, and FT4 produced by the thyroid glands were dramatically decreased, whereas TSH was excessively elevated, in the mutants (n = 10) compared with the WT individuals (n = 10; $^{**}P < .01$). EF hand, the position of calcium binding; FAD binding, flavin adenine dinucleotide–binding motif; H, heme-binding site; Mut, mutant; NADPH binding, nicotinamide adenine dinucleotide phosphate–binding motif; TM, transmembrane domain.

of H_2O_2 in the thyroid tissues, thymuses, and kidneys of both WT and mutant pigs. The results revealed that basal H_2O_2 concentration in the mutant thyroids was significantly decreased compared with that in the WT thyroids but not in the thymuses and kidneys (Figure 2B), suggesting that H_2O_2 deficiency directly affects the thyroid and unlikely has a direct effect on the thymus or other tissues exhibiting a relatively low *DUOX2* expression level. DUOX2 interacts with the activator protein DUOXA2 to produce H_2O_2,[30] which is the essential substrate of thyroperoxidase for iodide oxidation and iodination of thyroglobulin, the rate-limiting step in TH biosynthesis.[31,32] Therefore, HeLa cells were cotransfected with either WT or D409G *DUOX2* porcine complementary DNAs (cDNAs) in the presence of *DUOXA2*

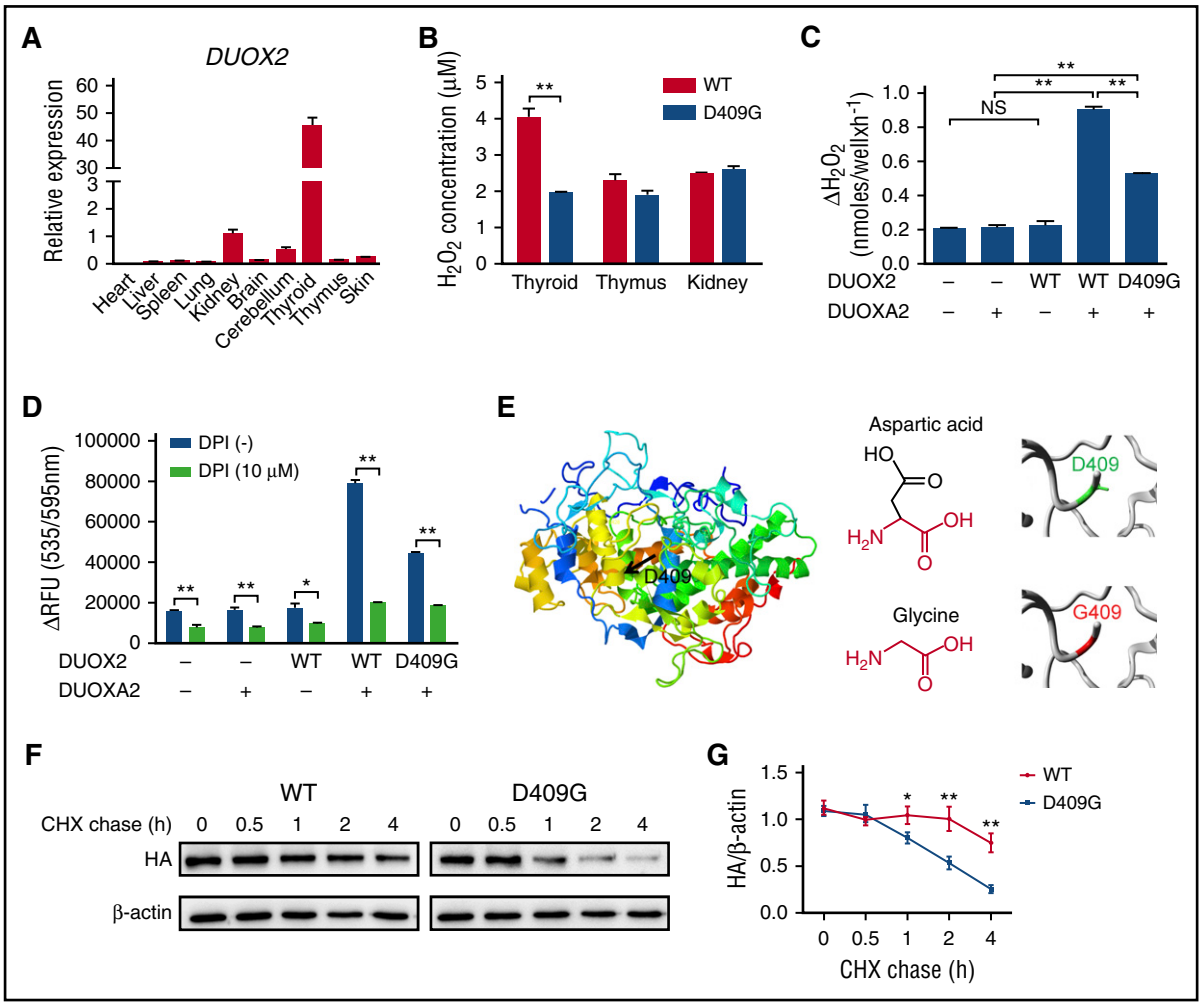

Figure 2. The loss-of-function p.D409G mutation hindered H_2O_2 production. (A) *DUOX2* mRNA was found to be abundant in the thyroids by qRT-PCR. (B) H_2O_2 concentrations in mutant thyroid tissues (n = 6) were more than twofold lower than those in WT tissues (n = 6) (**$P < .01$). No alterations in H_2O_2 concentrations were found in the thymuses and kidneys (WT, n = 6; D409G, n = 6; $P > .05$). (C) H_2O_2-producing capacities in HeLa cells were evaluated by cotransfection with either WT or D409G *DUOX2* porcine cDNAs in the presence of *DUOXA2*. The cotransfection of D409G *DUOX2* with *DUOXA2* resulted in only 50% of the H_2O_2 being produced compared with WT (**$P < .01$; the data presented are the means ± standard error [SE] of 3 independent experiments). (D) The H_2O_2 release triggered by WT and D409G mutant DUOX2 was completely blocked by incubation with DPI. *$P < .05$, **$P < .01$; the data presented are the means ± SE of 3 independent experiments. (E) The potential structural impact of the D409G mutation (arrow) on DUOX2 was predicted by the 3D protein structure using SWISS-MODEL and HOPE. The negatively charged aspartic acid is converted into neutral glycine. (F) Protein stability assays with CHX chase showed a more rapid decrease in the amount of D409G protein in comparison with WT protein at the examined time points after 0.5 hours. (G) Western blot signals were measured using ImageJ software, and obtained values of hemagglutinin (HA)/β-actin from 3 replications were graphed to produce degradation curves (*$P < .05$, **$P < .01$). In addition to the specific notes, all data are presented as the means ± SD. DPI, diphenyleneiodonium; NS, not significant; RFU, relative fluorescence unit.

to further confirm whether the decreased H_2O_2 production was caused by the D409G mutation directly. The results showed that cotransfection of WT *DUOX2* with *DUOXA2* significantly increased H_2O_2 production (Figure 2C). In contrast, cotransfection of D409G *DUOX2* with *DUOXA2* produced only 50% of the H_2O_2 compared with the WT level, indicating that the mutation impairs the ability of DUOX2 to generate H_2O_2 (Figure 2C). The H_2O_2 production triggered by DUOX2 was completely blocked by incubation with diphenyleneiodonium, a flavoprotein inhibitor (Figure 2D). To explore the function of the D409G mutation in *DUOX2*, real-time quantitative reverse transcriptase polymerase chain reaction (qRT-PCR) was performed and the results revealed that the D409G mutation did not alter the *DUOX2* expression at the transcript level (supplemental Figure 4A). The immunofluorescence data showed that the D409G mutation did not affect the subcellular localization pattern of DUOX2 in Hela cells (supplemental Figure 4B). Furthermore, the effect of the D409G mutation on the DUOX2 protein 3-dimensional (3D) structure was predicted, and the results suggested that the WT residue was converted from a negatively charged residue to a neutral residue, which may disturb the required rigidity of the protein (Figure 2E). We further performed protein stability assays on 293T cells transfected with WT and HA-D409G *DUOX2* vectors using cycloheximide (CHX) chase. The results showed a more rapid decrease in the amount of D409G protein, in comparison with WT DUOX2 protein, from 0.5 hours after CHX treatment (Figure 2F), with <20% of the mutant protein being present compared with >70% of WT DUOX2 protein after 4 hours of treatment (Figure 2G). Taken together, the findings demonstrated that the D409G mutation causing DUOX2 instability impairs H_2O_2 generation in the thyroids of $DUOX2^{D409G/D409G}$ pigs, which resulted in TH synthesis failure.

CH pigs display phenotypic hallmarks of anemia and immunodeficiency

CH is frequently accompanied by anemia and immunodeficiency.[3-8] Peripheral blood smears revealed that the mutants exhibited a markedly

higher number of nucleated red blood cells (NRBCs) per 100 white blood cell (WBC) count (187.0 ± 18.01) than did the WT group (3.7 ± 2.93) (Figure 3A). Simultaneously, routine blood tests revealed significantly lower levels of red blood cell count, hemoglobin (HGB), hematocrit, and red blood cell distribution width in the mutant pigs (Figure 3B), whereas WBC count (Figure 3B, corrected by NRBCs[33]), mean corpuscular volume, mean corpuscular HGB, and mean corpuscular HGB concentration were normal in these pigs (supplemental Figure 5A). These data suggested that compensatory erythropoiesis may occur due to severe anemia.[33] Furthermore, we also detected the lymphocyte subsets in peripheral blood using multicolor flow cytometry (supplemental Figure 5B-D). Compared with WT pigs, *DUOX2*$^{D409G/D409G}$ mutants had significantly lower levels of $CD3^+$ T cells, $CD4^+CD8^+$ cells, $CD4^-CD8^-$ cells, and the $CD3^+$ subpopulation of $CD4^+CD8^-$ helper T cells (Figure 3C); no significant differences were observed in $CD4^-CD8^+$ cytotoxic T lymphocytes (Figure 3C) and $CD21^+$ B cells (supplemental Figure 5D).

To determine whether the hematopoietic organs were affected in the mutant pigs, we further performed histopathological analysis. The thymuses from *DUOX2*$^{D409G/D409G}$ piglets showed that the lobules were atrophied, and the number of thymocytes was remarkably decreased compared with that in their WT littermates (Figure 3D, top left panel). The periarterial lymphatic sheaths from the mutant spleens became hypoplastic, and the white pulps almost disappeared. The number of lymphocytes was also remarkably reduced in the mutant pigs (Figure 3D bottom left panel). Our data also showed that the mutant pigs exhibited atrophy of the thymuses and enlargement of the spleens (Figure 3D, right panel). Together, these results demonstrated that severe anemia and T lymphopenia were observed in *DUOX2*$^{D409G/D409G}$ piglets, which manifest many clinical features of human CH.

KLF9 is downregulated in mutant pigs and is a direct target gene of TH

To better understand the molecular mechanism underlying the co-occurrence of CH and anemia as well as immunodeficiency, we conducted RNA sequencing (RNA-seq) analysis in the thymuses. A volcano plot was constructed to show the top differentially expressed genes (DEGs) and transcripts (Figure 4A). The hierarchical clustering analysis based on these DEGs further demonstrated a clearly distinct expression pattern between *DUOX2*$^{D409G/D409G}$ mutant and WT pigs (supplemental Figure 6A). Among these DEGs, *KLF9* was the most dramatically downregulated gene in *DUOX2*$^{D409G/D409G}$ pigs (Figure 4A), as further confirmed by qRT-PCR (Figure 4B).

Because *KLF9* is regulated by T3 in the rodent brain through the TR/KLF9 axis[34] and is markedly downregulated in the hypothyroid porcine thymuses, which are the organs for T-lymphocyte generation, we hypothesized that *KLF9* may play a vital role in hematopoiesis under the regulation of TH. The expression pattern of different TR isoforms showed that, *THRB*, but not *THRA*, expression was significantly downregulated in the hypothyroid thymuses. A similar pattern was also observed in the spleens (Figure 4B), suggesting that *KLF9* expression might be positively regulated by *THRB* in the thymus and spleen tissues. To determine whether T3 induces *KLF9* expression in hematopoietic cells, K562, a erythroleukemic cell line compatible with the nature of erythroid cells,[35] was treated with T3 and the expression of *KLF9* as well as TRs was measured using qRT-PCR. Our data demonstrated that T3 treatment caused upregulation of *KLF9* in a dose- and time-dependent manner (Figure 4C; supplemental Figure 6B), and the simultaneous upregulation of both *THRA* and *THRB* (Figure 4C) suggested that T3 may regulate *KLF9* via TRs in hematopoietic cells. These data also indicated that *KLF9* might be regulated in different organs or cells by different TRs.

TRs regulate their target genes via the binding of specific TH response elements (*TRE*s) in the promoter region.[36] Bioinformatics analysis indicated that there are 7 putative *TRE*s in 2 regions (R1 and R2) of the porcine *KLF9* promoter sequence, based on the human and mouse *TRE*s[36] (Figure 4D; supplemental Table 5). To further confirm that porcine *KLF9* was regulated directly by TRs through the binding of the putative *TRE*s, plasmids of R1 or R2 and porcine TR isoforms were cotransfected in 293T cells. After 24 to 48 hours, a dual-luciferase reporter assay suggested that the putative *TRE*s that bind to TRs are located in R2 (Figure 4E). The luciferase reporter assay further revealed that only the mutated TRE7 (mTRE7) cotransfected with *THRA* showed significantly decreased luciferase activity, suggesting that TRE7 might be the functional putative *TRE* (Figure 4F). To further confirm this finding, TRE7 or mTRE7 and TR isoforms were cotransfected. As expected, the WT TRE7 responded to TRs (Figure 4G) in a dose-dependent manner (supplemental Figure 6C), whereas mTRE7 did not (Figure 4G), further confirming that TRs directly regulate *KLF9* via KLF9-TRE7. Collectively, *KLF9* is a direct target gene of TH and is regulated in a TR-dependent manner.

klf9 plays a vital role in hematopoiesis downstream of the TH/TR axis

To determine whether *KLF9* functions as the downstream effector of the TH/TR axis during regulation of hematopoiesis in vivo, we used a zebrafish model. First, we examined the expression patterns of *thraa*, *thrab*, *thrb* (orthologous genes of TRs in zebrafish), and *klf9* during embryogenesis (supplemental Figure 7A). The whole-mount in situ hybridization (WISH) data showed that *thraa*, *thrb*, and *klf9* were expressed ubiquitously from the 1-cell stage onwards. To examine whether *klf9* is regulated by TH in zebrafish, we treated zebrafish embryos with T3 at 0.8 μg/mL from the tail-bud stage to 3 days postfertilization (dpf). The qRT-PCR analysis showed that the expression of *klf9*, *thraa*, *thrab*, and *thrb* was significantly upregulated in the T3 treatment group compared with the control group (Figure 5A). In contrast, we treated the embryos with propylthiouracil, the inhibitor of TH, at 4 μg/mL and 8 μg/mL, respectively, from embryonic stage (10 hours postfertilization [hpf]) for 7 days and found that *klf9* and *thrb* were downregulated in the propylthiouracil-treated embryos compared with the control (supplemental Figure 7B). Taken together, these data support that *klf9* is regulated by TH/TR signaling in zebrafish.

To evaluate the role of *klf9* in hematopoiesis, a *klf9* antisense MO was designed to knock down endogenous *klf9* expression. The lack of green fluorescence protein (GFP) expression in embryos coinjected with the *klf9*-pEGFP-N1 plasmid and the *klf9* MO demonstrated that the *klf9* MO worked efficiently (supplemental Figure 7C). We found that the expression levels of hematopoietic markers, including *gata1*, *scl*, *cmyb*, *lyz*, *mfap4*, and *be2-globin*, were normal in *klf9* MO-injected embryos (morphants) compared with controls at the 5-, 10-somite stages and at 24, 36 hpf (supplemental Figure 7D-F), indicating that the initiation of primitive hematopoiesis was not impaired. However, at 48 hpf, *O*-dianisidine staining revealed that the number of mature erythroid cells was decreased in *klf9* morphants (Figure 5B upper panel). The WISH data also indicated that erythroid marker *be2-globin* expression was reduced at 48 hpf, when *klf9* was knocked down (Figure 5B lower panel). Furthermore, the *Tg*(*gata1*:*dsRed*) line was used to observe hematopoietic cells in vivo, and confocal imaging showed that *gata1*$^+$ cells were significantly reduced in the morphants compared with the controls at 24 hpf, 3 dpf, and 4 dpf (Figure 5C). The blood-smear and Giemsa-staining results showed that the ratio of mature red blood cells was clearly reduced in *klf9* morphants compared with controls at 4 dpf

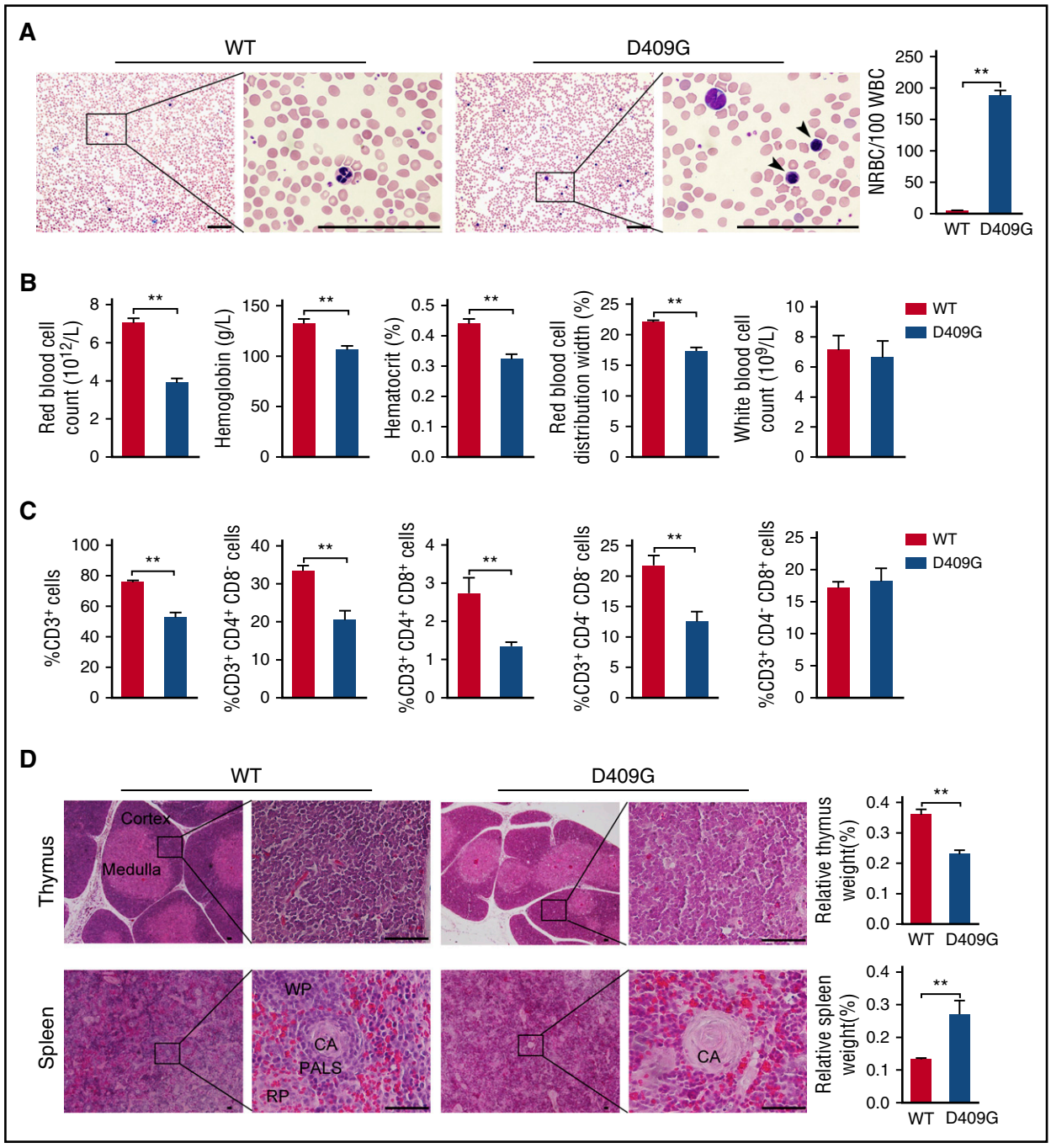

Figure 3. The D409G pigs displayed severe anemia and immunodeficiency. (A) The Wright-Giemsa staining of peripheral blood smears showed that the mutants exhibited a higher number of NRBCs (arrowheads) per 100 WBCs than did the WT group (WT, n = 7; D409G, n = 6). Scale bars, 50 μm. The quantification of NRBCs per 100 WBCs on the right showed that the number of NRBCs in D409G pigs was markedly higher (187.0 ± 18.01) than that of WT pigs (3.7 ± 2.93). $^{**}P < .01$. (B) The D409G pigs exhibited anemia with significantly lower levels of red blood cells (RBCs), HGB, and hematocrit (HCT) (WT, n = 15; D409G, n = 10; $^{**}P < .01$), whereas WBC count was normal (WT, n = 7; D409G, n = 6; $P > .05$). (C) The D409G mutants had lower levels of $CD3^+$ T cells, $CD4^+CD8^+$ cells, $CD4^-CD8^-$ cells, and the $CD3^+$ subpopulation of $CD4^+CD8^-$ helper T cells ($^{**}P < .01$), and no significant differences were observed in $CD4^-CD8^+$ cytotoxic T lymphocytes ($P > .05$) compared with WT pigs (WT, n = 15; D409G, n = 10). (D) The H&E staining results revealed atrophied lobules and decreased thymocytes in the thymuses (top left panel) of D409G mutants; the mutant spleens (bottom left panel) exhibited periarterial lymphatic sheath (PALS) and indistinguishable white pulp (WP) and red pulp (RP) compared with the WT spleens (central artery [CA]). The number of lymphocytes was also remarkably reduced in the spleens of mutant pigs. Scale bars, 50 μm. The relative spleen weight was increased in D409G pigs, whereas the thymus weight was notably decreased compared with that of WT pigs (right panel) (WT, n = 15; D409G, n = 10; $^{**}P < .01$). The weights of organs were normalized by total body weight. The data are presented as the means ± SD.

(Figure 5D-E). In addition, the *klf9* expression in *gata1*$^+$ cells sorted from embryos at 3 dpf induced by 0.8 μg/mL T3 treatment was significantly increased, suggesting that *klf9* is involved in TH deficiency-related erythropoiesis defects directly (Figure 5F). Meanwhile, we performed qRT-PCR to detect *ae1-globin*, *pu.1*, and *lck* gene expression at 4 dpf. The results showed that expression of *ae1-globin* (erythroid) and *lck* (lymphoid) decreased significantly whereas the expression of *pu.1* (myeloid) was not changed in *klf9* morphants

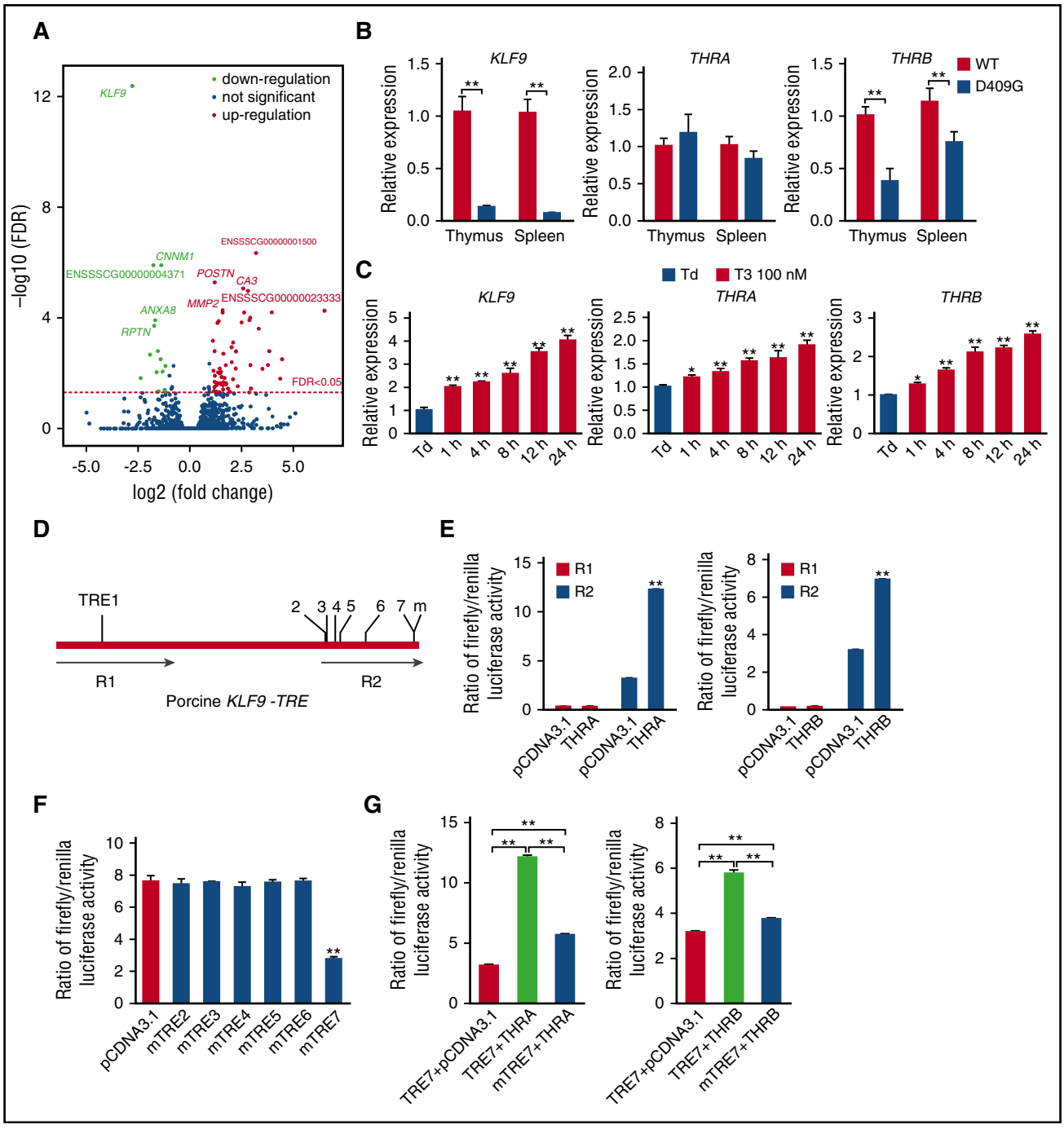

Figure 4. Porcine *KLF9* is a direct target gene of TH. (A) The volcano plot revealed that 78 genes were dysregulated, including *KLF9*, which was predominantly downregulated in the thymuses of hypothyroid mutants. (B) *KLF9* and *THRB* mRNA expression were notably decreased in the thymuses and spleens of hypothyroid pigs compared with those of their WT littermates (WT, n = 15; D409G, n = 10; $^{**}P < .01$). (C) K562 cells were treated with 100 nM T3 for 1 to 24 hours, and *KLF9* expression was measured by qRT-PCR. The data revealed that T3 significantly upregulated *KLF9*, as well as *THRA* and *THRB*. The data are presented as the means ± SD of 3 replications ($^{*}P < .05$, $^{**}P < .01$). (D) Schematic representation of the porcine *KLF9*-truncated promoter. Seven putative *TRE*s located in 2 regions (R1 and R2) were predicted. (E) Luciferase assay of the reporters containing R1 or R2 of the truncated *KLF9* promotor in 293T cells. Compared with the cells cotransfected with R2 and empty vector (pcDNA3.1), both *THRA* and *THRB* markedly enhanced the luciferase activity of R2, whereas R1 had no luciferase expression activity ($P > .05$). (F) The luciferase activity assay revealed that only mTRE7 showed significantly decreased luciferase activity after cotransfection with *THRA*, compared with the other mTRE2-6. (G) The luciferase activity of TRE7 was significantly elevated in response to any TR isoform, whereas decreased expression of the mutated TRE7 was observed in the presence of both TR isoforms. The data are presented as the means ± SD of 3 replications ($^{**}P < 0.01$). FDR, false discovery rate; m, mutation; Td, TH deficiency.

(Figure 5G). Furthermore, the WISH result of *rag1* and confocal imaging of *coro1a*$^{+}$ cells in the thymus region indicated that T lymphocytes were reduced at 4 and 5.5 dpf upon *klf9* knockdown (Figure 5H-I). To explore the reasons for hematopoietic cell defects, we performed terminal deoxynucleotidyltransferase-mediated dUTP nick end labeling (TUNEL) assays to detect cell apoptosis and found that the number of apoptotic signals was increased in *klf9* morphants compared with controls (Figure 5J-K). Moreover, the expression levels of genes associated with cell cycle and cell division were decreased significantly in *klf9* morphants at 5 dpf by the qRT-PCR result (Figure 5L). However,

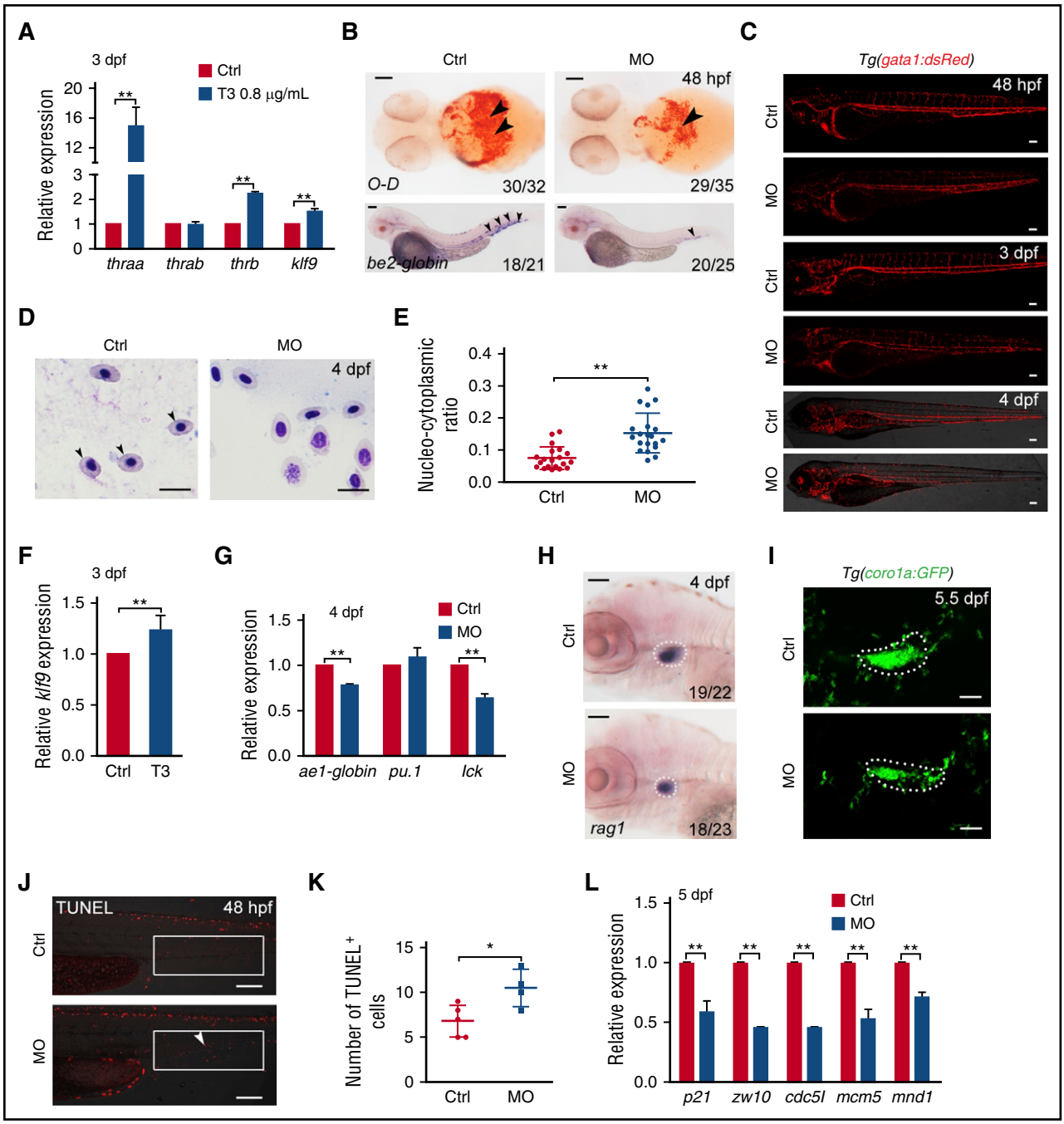

Figure 5. *klf9* mediates the TH/TR axis to regulate hematopoiesis. (A) The qRT-PCR results showed that the expression levels of *klf9*, *thraa*, and *thrb* were significantly upregulated in the T3-treated zebrafish embryos compared with the controls at 3 dpf (means ± SD; $^{**}P < .01$; n = 3). (B) *O*-dianisidine (O-D) staining of hemoglobin and *be2-globin* expression by WISH revealed that mature erythrocytes were decreased in *klf9* morphants compared with control embryos at 48 dpf. RBCs are indicated by arrowheads. Scale bar, 100 μm. (C) Confocal imaging of *Tg*(*gata1*:*dsRed*) showing fewer *gata1*:*dsRed* cells in *klf9* morphants at 48 hpf, 3 dpf, and 4 dpf. Scale bar, 100 μm. (D) Blood smear and Giemsa staining. At 4 dpf, the size and nucleocytoplasmic ratio of RBCs from *klf9* morphants were increased compared with those from controls. The arrowhead marks the mature RBCs. Scale bar, 10 μm. (E) Scatter plots of the nucleocytoplasmic ratio in control and *klf9* morphants (means ± SD; $^{**}P < .01$; n = 20). (F) The qRT-PCR result displayed that *klf9* expression was increased in *gata1*$^{+}$ cells after T3 treatment from 10 hpf to 3 dpf (means ± SD; $^{**}P < .01$; n = 5). (G) The qRT-PCR results showed that *ae1-globin* and *lck* expression levels were significantly decreased in *klf9* morphants compared with controls at 4 dpf (means ± SD; $^{**}P < .01$; n = 3). (H) WISH result showed that the expression of T-cell marker *rag1* was decreased in *klf9* morphants at 4 dpf. The white dashed lines indicate the thymus region. Scale bars, 100 μm. (I) Confocal imaging of *Tg*(*coro1a*:*GFP*) showed that T cells in the thymus (dashed line) were decreased in *klf9* morphants compared with controls at 5.5 dpf. Scale bars, 40 μm. (J-K) The quantification of apoptotic cells in the caudal hematopoietic tissue (white boxes) showed that the number of TUNEL^{+} cells (arrowhead) was 1.5-fold higher in morphants than that in controls at 2 dpf (means ± SD; $^{*}P < .05$; Ctrl, n = 5; MO, n = 4). Scale bars, 100 μm. (L) The qRT-PCR results showed that the expression levels of cell division–associated genes were downregulated in *klf9* morphants at 5 dpf (means ± SD; $^{**}P < .01$; n = 3). Ctrl, control; MO, *klf9* MO.

5-bromo-2′-deoxyuridine assays showed no obvious differences in the morphants compared with the controls (supplemental Figure 7G). Taken together, these results demonstrated that *klf9* is involved in hematopoietic development including erythroid maturation, T lymphopoiesis through the regulation of cell apoptosis, and cell division during zebrafish embryogenesis.

Discussion

Animal models are crucial for deciphering disease pathogenesis and developing novel therapeutic agents and treatments.[37] The ideal animal model should resemble not only a human disease phenotype but also its underlying causality. In this circumstance, pigs have anatomical, physiological, and genomic characteristics that are similar to humans, which make them highly suitable for modeling human diseases, such as cardiovascular diseases, neurodegenerative diseases, cystic fibrosis, and diseases of the eyes.[38] More importantly, porcine thyroid extract has been widely used for treatment of CH,[39] and pigs and humans are known to share a high degree of homology in TH metabolism,[22] which implicates that pigs might be suitable animals for the CH studies. In this work, a CH pig model was created by ENU mutagenesis for the first time. The causative mutation was mapped in the *DUOX2* gene and was further verified by CRISPR/Cas9 system–mediated deletion.

DUOX2 mutations are one of the leading genetic causes of CH. Since the first mutation in *DUOX2* was discovered in subjects with CH,[25] over 30 mutations have been identified in patients with CH (until 2014).[40] The $DUOX2^{D409G/D409G}$ pigs displayed overt goiter and significantly decreased TH, which mimicked the phenotypic hallmarks of patients with severe CH. Although many organ systems may be affected in hypothyroidism, the hematopoietic system is the primary one,[9] as was first reported in the 1940s.[41] In the mutant pigs, severe anemia and T lymphopenia were also observed, which provides us a suitable animal model to decipher the underlying molecular mechanism for the co-occurrence of CH and anemia or immunodeficiency.

Hematopoiesis is the process by which distinct blood cells, such as erythrocytes, T, and B lymphocytes acquire defining phenotypes as a result of coordinated, cell-specific gene expression mediated by specific transcription factors.[42] TRs are expressed in hematopoietic progenitor cells, and TR expression can be regulated by hypo- and hyperthyroidism status, indicating that TH plays vital roles in hematopoiesis.[16,17] Thus, it has been suggested that disturbance of the thyroid state can cause hematologic disorders. In the current study, *KLF9* was dramatically downregulated in pigs with CH, which prompted us to investigate its role in hematopoiesis under the regulation of the TH.

There are 17 Krüppel-like factors (KLFs) that act as transcription factors, and most of them participate in hematopoiesis including erythropoiesis, lymphopoiesis, and the formation and functions of monocytes and macrophages.[43] Previous studies[24,43,44] reported that *KLF*s 1, 2, 4, 5, 6, 8, 12, and 13 regulate erythropoiesis, whereas *KLF10* and *KLF13* have important functions in the development of T lymphocytes involving the immune system and inflammatory responses. *KLF9* was reported to be a direct TH response gene,[34] however, much less is known about its role in hematopoiesis, and only 1 study reported that *KLF9* was upregulated by T3 in human red blood cell progenitors.[45] On the other hand, *KLF9* was reported to play a key role in rodent neuronal morphogenesis downstream of TRs.[36,46,47] The TR/KLF9 axis is also active in the proliferation and differentiation of nonneuronal cell types of hepatocytes and pluripotent stem cells.[48] Moreover, *KLF9* is highly expressed in the thymus[43] and in human erythroid cells.[45] In the current study, we found that TH upregulates *KLF9* via TRs binding the *TREs* in the *KLF9* promoter. The results of *klf9* knockdown in zebrafish embryos confirmed our hypothesis that *klf9* is involved in hematopoietic development including erythroid maturation and T lymphopoiesis. To our knowledge, this study provides the first experimental evidence that TH impacts hematopoiesis via *KLF9*.

Beyond uncovering the hematopoietic function of *KLF9* downstream of the TH/TR axis, our finding regarding *KLF9* may shed light on the treatment protocol for thyroid disease. The most common treatment of hypothyroidism is T4 replacement or T4-T3 combination therapy.[49] Despite symptomatic improvement with both treatments in patients to some extent,[50] some patients remain unsatisfied with the persistence of specific symptoms or a failure to regain a normal sense of well-being.[51,52] One study reported that even when hormone replacement therapy was performed soon after birth, it was difficult to maintain steady and normal levels of hematological parameters,[3] suggesting that the growth potential of the hematopoietic tissue might be irreversibly limited by its period of severe hypothyroidism and that the TH supplement alone is not sufficient in certain patients with irreversible lesions. Therefore, the combination therapy of TH replacement and the development of medicines for regulating hematopoietic target genes might be considered in clinic.

In summary, in this study, we have created a pig mutant that can model human CH, and our results support that *KLF9* acts as a mediator between the thyroid axis and hematopoiesis. These findings may provide a promising alternative for therapeutic intervention in hypothyroid patients with anemia and immunodeficiency.

Acknowledgments

The authors thank all of the personnel at the Beijing Farm Animals Research Center, the Chinese Academy of Sciences, and the Chinese Swine Mutagenesis Consortium who are not listed as coauthors of this paper for their assistance.

This work was supported by the Strategic Priority Research Program of the Chinese Academy of Sciences (XDA08000000), the National Transgenic Project of China (2016ZX08009003-006-007), the National Natural Science Foundation of China (81671274, 31425016, 31402045, 31601008, 81530004, and 81770789), the National Basic Research Program of China (2011CBA0100, 2011CB944100, 2011BAI15B02, 2012BAI39B04, and 2016YFA0100500), and the National High Technology Research and Development Program of China (2012AA020602).

Authorship

Contribution: J.Z., F.L., and H. Wei conceived the project with input from A.M., Q. Zhou, and H. Wang; all experiments were performed by Y.Z., Y.X., J.H., Q.H., T.H., Q.J., Xianlong Wang, G.Q., J.Y., Xiao Wang, Q. Zheng, R.Z., Y.L., A.L., and N.Z. under the supervision of J.Z. and F.L.; C.C. performed the GWLS, WGS, RNA-sequencing, and data analyses, and conducted the bioinformatics analyses; G.S. and Y.Z. analyzed the histopathological results; H.Y. and Z.L. contributed critical experiment materials; and J.Z., F.L., Y.Z., Y.X., C.C., and Y.W. wrote the manuscript.

Conflict-of-interest disclosure: The authors declare no competing financial interests.

Correspondence: Hong Wei, Department of Laboratory Animal Science, College of Basic Medical Sciences, Third Military Medical University, 29 Gaotanyan Rd, Shapingba District, Chongqing 400038, China; e-mail: weihong63528@163.com; Feng Liu, State Key Laboratory of Membrane Biology, Institute of Zoology, Chinese Academy of Sciences, 1 Beichen West Rd, Chaoyang District, Beijing 100101, China; e-mail: liuf@ioz.ac.cn; and Jianguo Zhao, State Key Laboratory of Stem Cell and Reproductive Biology, Institute of Zoology, Chinese Academy of Sciences, 1 Beichen West Rd, Chaoyang District, Beijing 100101, China; e-mail: zhaojg@ioz.ac.cn.

References

1. Wassner AJ, Brown RS. Hypothyroidism in the newborn period. *Curr Opin Endocrinol Diabetes Obes*. 2013;20(5):449-454.
2. Hollenberg AN, Choi J, Serra M, Kotton DN. Regenerative therapy for hypothyroidism: mechanisms and possibilities. *Mol Cell Endocrinol*. 2017;445:35-41.
3. Franzese A, Salerno M, Argenziano A, Buongiovanni C, Limauro R, Tenore A. Anemia in infants with congenital hypothyroidism diagnosed by neonatal screening. *J Endocrinol Invest*. 1996; 19(9):613-619.
4. Kazemi-Jahromi M, Shahriari-Ahmadi A, Samedanifard S-H, Doostmohamadian S, Abdolahpoor E, Allameh SF. The association between hypothyroidism and anemia: a clinical study. *Int J Hematol Oncol Stem Cell Res*. 2010; 4(3):6-9.
5. Das P, Sahu D, Ramalingam R, Venkatesh S, Dhandapany G. Congenital hypothyroidism presenting with severe neonatal anaemia. *Curr Pediatr Res*. 2015;19(1-2):79-80.
6. Watanabe K, Iwatani Y, Hidaka Y, Watanabe M, Amino N. Long-term effects of thyroid hormone on lymphocyte subsets in spleens and thymuses of mice. *Endocr J*. 1995;42(5):661-668.
7. Pillay K. Congenital hypothyroidism and immunodeficiency: evidence for an endocrine-immune interaction. *J Pediatr Endocrinol Metab*. 1998;11(6):757-761.
8. Jafarzadeh A, Poorgholami M, Izadi N, Nemati M, Rezayati M. Immunological and hematological changes in patients with hyperthyroidism or hypothyroidism. *Clin Invest Med*. 2010;33(5): E271-E279.
9. Erdogan M, Kösenli A, Ganidagli S, Kulaksizoglu M. Characteristics of anemia in subclinical and overt hypothyroid patients [published correction appears in *Endocr J*. 2013;60(4):541]. *Endocr J*. 2012;59(3):213-220.
10. Labourier E. Utility and cost-effectiveness of molecular testing in thyroid nodules with indeterminate cytology. *Clin Endocrinol (Oxf)*. 2016;85(4):624-631.
11. Thompson CC, Weinberger C, Lebo R, Evans RM. Identification of a novel thyroid hormone receptor expressed in the mammalian central nervous system. *Science*. 1987;237(4822): 1610-1614.
12. Bochukova E, Schoenmakers N, Agostini M, et al. A mutation in the thyroid hormone receptor alpha gene [published correction appears in *N Engl J Med*. 2012;367(15):1474]. *N Engl J Med*. 2012; 366(3):243-249.
13. Gauthier K, Chassande O, Plateroti M, et al. Different functions for the thyroid hormone receptors TRalpha and TRbeta in the control of thyroid hormone production and post-natal development. *EMBO J*. 1999;18(3):623-631.
14. Kendrick TS, Payne CJ, Epis MR, et al. Erythroid defects in TRalpha-/- mice. *Blood*. 2008;111(6): 3245-3248.
15. Arpin C, Pihlgren M, Fraichard A, et al. Effects of T3R alpha 1 and T3R alpha 2 gene deletion on T and B lymphocyte development. *J Immunol*. 2000;164(1):152-160.
16. Grymuła K, Paczkowska E, Dziedziejko V, et al. The influence of 3,3′,5-triiodo-L-thyronine on human haematopoiesis. *Cell Prolif*. 2007;40(3): 302-315.
17. Kawa MP, Grymula K, Paczkowska E, et al. Clinical relevance of thyroid dysfunction in human haematopoiesis: biochemical and molecular studies. *Eur J Endocrinol*. 2010;162(2):295-305.
18. Prather RS, Shen M, Dai Y. Genetically modified pigs for medicine and agriculture. *Biotechnol Genet Eng Rev*. 2008;25:245-265.
19. Rogers CS, Stoltz DA, Meyerholz DK, et al. Disruption of the CFTR gene produces a model of cystic fibrosis in newborn pigs. *Science*. 2008; 321(5897):1837-1841.
20. Meurens F, Summerfield A, Nauwynck H, Saif L, Gerdts V. The pig: a model for human infectious diseases. *Trends Microbiol*. 2012;20(1):50-57.
21. Fan N, Lai L. Genetically modified pig models for human diseases. *J Genet Genomics*. 2013;40(2): 67-73.
22. Wassen FW, Klootwijk W, Kaptein E, Duncker DJ, Visser TJ, Kuiper GG. Characteristics and thyroid state-dependent regulation of iodothyronine deiodinases in pigs. *Endocrinology*. 2004;145(9): 4251-4263.
23. Hai T, Cao C, Shang H, et al. Pilot study of large-scale production of mutant pigs by ENU mutagenesis. *eLife*. 2017;6:e26248.
24. Xue Y, Gao S, Liu F. Genome-wide analysis of the zebrafish Klf family identifies two genes important for erythroid maturation. *Dev Biol*. 2015;403(2): 115-127.
25. Moreno JC, Bikker H, Kempers MJ, et al. Inactivating mutations in the gene for thyroid oxidase 2 (THOX2) and congenital hypothyroidism. *N Engl J Med*. 2002;347(2): 95-102.
26. Vigone MC, Fugazzola L, Zamproni I, et al. Persistent mild hypothyroidism associated with novel sequence variants of the DUOX2 gene in two siblings. *Hum Mutat*. 2005;26(4):395.
27. Ohye H, Fukata S, Hishinuma A, et al. A novel homozygous missense mutation of the dual oxidase 2 (DUOX2) gene in an adult patient with large goiter. *Thyroid*. 2008;18(5):561-566.
28. Cangul H, Aycan Z, Kendall M, et al. A truncating DUOX2 mutation (R434X) causes severe congenital hypothyroidism. *J Pediatr Endocrinol Metab*. 2014;27(3-4):323-327.
29. Grasberger H, De Deken X, Miot F, Pohlenz J, Refetoff S. Missense mutations of dual oxidase 2 (DUOX2) implicated in congenital hypothyroidism have impaired trafficking in cells reconstituted with DUOX2 maturation factor. *Mol Endocrinol*. 2007; 21(6):1408-1421.
30. Zamproni I, Grasberger H, Cortinovis F, et al. Biallelic inactivation of the dual oxidase maturation factor 2 (DUOXA2) gene as a novel cause of congenital hypothyroidism. *J Clin Endocrinol Metab*. 2008;93(2):605-610.
31. De Deken X, Wang D, Many MC, et al. Cloning of two human thyroid cDNAs encoding new members of the NADPH oxidase family. *J Biol Chem*. 2000;275(30):23227-23233.
32. Song Y, Ruf J, Lothaire P, et al. Association of duoxes with thyroid peroxidase and its regulation in thyrocytes. *J Clin Endocrinol Metab*. 2010; 95(1):375-382.
33. Constantino BT, Cogionis B. Nucleated RBCs: significance in the peripheral blood film. *Lab Med*. 2000;31(4):223-229.
34. Denver RJ, Ouellet L, Furling D, Kobayashi A, Fujii-Kuriyama Y, Puymirat J. Basic transcription element-binding protein (BTEB) is a thyroid hormone-regulated gene in the developing central nervous system. Evidence for a role in neurite outgrowth. *J Biol Chem*. 1999;274(33): 23128-23134.
35. Andersson LC, Nilsson K, Gahmberg CG. K562–a human erythroleukemic cell line. *Int J Cancer*. 1979;23(2):143-147.
36. Denver RJ, Williamson KE. Identification of a thyroid hormone response element in the mouse Kruppel-like factor 9 gene to explain its postnatal expression in the brain. *Endocrinology*. 2009; 150(8):3935-3943.
37. McGonigle P, Ruggeri B. Animal models of human disease: challenges in enabling translation. *Biochem Pharmacol*. 2014;87(1): 162-171.
38. Yao J, Huang J, Zhao J. Genome editing revolutionize the creation of genetically modified pigs for modeling human diseases. *Hum Genet*. 2016;135(9):1093-1105.
39. Hennessey JV. Historical and current perspective in the use of thyroid extracts for the treatment of hypothyroidism. *Endocr Pract*. 2015;21(10): 1161-1170.
40. Jin HY, Heo SH, Kim YM, et al. High frequency of DUOX2 mutations in transient or permanent congenital hypothyroidism with eutopic thyroid glands. *Horm Res Paediatr*. 2014;82(4):252-260.
41. Levine B, Rosenberg DV. Aplastic anemia during the treatment of hyperthyroidism with tapazole. *Ann Intern Med*. 1954;41(4):844-848.
42. Shivdasani RA, Orkin SH. The transcriptional control of hematopoiesis. *Blood*. 1996;87(10): 4025-4039.
43. McConnell BB, Yang VW. Mammalian Krüppel-like factors in health and diseases. *Physiol Rev*. 2010;90(4):1337-1381.
44. Xue Y, Lv J, Zhang C, Wang L, Ma D, Liu F. The vascular niche regulates hematopoietic stem and progenitor cell lodgment and expansion via klf6a-ccl25b. *Dev Cell*. 2017;42(4):349-362.e4.
45. Gamper I, Koh KR, Ruau D, et al. GAR22: a novel target gene of thyroid hormone receptor causes growth inhibition in human erythroid cells. *Exp Hematol*. 2009;37(5):539-548.e4.
46. Martel J, Cayrou C, Puymirat J. Identification of new thyroid hormone-regulated genes in rat brain neuronal cultures. *Neuroreport*. 2002;13(15): 1849-1851.
47. Avci HX, Lebrun C, Wehrlé R, et al. Thyroid hormone triggers the developmental loss of axonal regenerative capacity via thyroid hormone receptor α1 and krüppel-like factor 9 in Purkinje cells. *Proc Natl Acad Sci USA*. 2012;109(35): 14206-14211.
48. Cvoro A, Devito L, Milton FA, et al. A thyroid hormone receptor/KLF9 axis in human hepatocytes and pluripotent stem cells. *Stem Cells*. 2015;33(2):416-428.
49. Jonklaas J, Bianco AC, Bauer AJ, et al; American Thyroid Association Task Force on Thyroid Hormone Replacement. Guidelines for the treatment of hypothyroidism: prepared by the American Thyroid Association Task Force On Thyroid Hormone Replacement. *Thyroid*. 2014; 24(12):1670-1751.
50. Okosieme OE. Thyroid hormone replacement: current status and challenges. *Expert Opin Pharmacother*. 2011;12(15):2315-2328.
51. Kaplan MM, Sarne DH, Schneider AB. In search of the impossible dream? Thyroid hormone replacement therapy that treats all symptoms in all hypothyroid patients. *J Clin Endocrinol Metab*. 2003;88(10):4540-4542.
52. Wiersinga WM. Do we need still more trials on T4 and T3 combination therapy in hypothyroidism? *Eur J Endocrinol*. 2009;161(6):955-959.

2017 130: 2161-2170
doi:10.1182/blood-2017-05-783043 originally published online September 25, 2017

Thyroid hormone regulates hematopoiesis via the TR-KLF9 axis

Ying Zhang, Yuanyuan Xue, Chunwei Cao, Jiaojiao Huang, Qianlong Hong, Tang Hai, Qitao Jia, Xianlong Wang, Guosong Qin, Jing Yao, Xiao Wang, Qiantao Zheng, Rui Zhang, Yongshun Li, Ailing Luo, Nan Zhang, Guizhi Shi, Yanfang Wang, Hao Ying, Zhonghua Liu, Hongmei Wang, Anming Meng, Qi Zhou, Hong Wei, Feng Liu and Jianguo Zhao

Blood (print ISSN 0006-4971, online ISSN 1528-0020), is published weekly by the American Society of Hematology, 2021 L St, NW, Suite 900, Washington DC 20036.